Highly porous activated carbon derived from papaya plant (stems and leaves) for superior adsorption of alizarin red s and methylene blue dyes from water

Mona Moheb[1], Ahmad M. El-Wakil[1], and Fathi S. Awad[1,2*]

[1]Chemistry Department, Faculty of Science, Mansoura University, Mansoura 35516, Egypt.
[2] Chemistry Department, Faculty of Science, New Mansoura University, New Mansoura 35712, Egypt.

Supporting Information

Table S1. Properties of methylene blue and alizarin red s

Dyes	**Molecular formula**	**Molecular structure**	**Three-dimensional molecular structure**	λ_{max}	**Molecular weight (g/mol)**	**Type of dye**
Methylene blue	$C_{16}H_{18}ClN_3S$	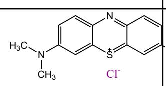	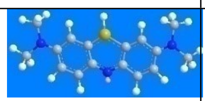	664nm	319.86 g/mol	Cationic dye
Alizarin red S	$C_{14}H_7NaO_7S$	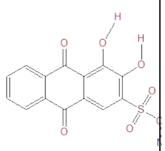	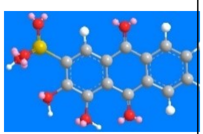	424nm (acidic medium) 520 nm (basic medium)	342.26 g/mol	anionic dye

Table S2: Surface characteristics of SAC and LAC.

Sample	**SAC**	**LAC**
BET surface area	1053.52 m²/g	441.671 m²/g
BJH adsorption surface area	266.186 m²/g	143.413 m²/g
Pore volume	0.785116 cc/g	0.338432 cc/g
Pore radius	1.92765 nm	1.9282 nm
DFT adsorption surface area	923.3446 m²/g	352.5197 m²/g
Pore Volume	1.1580 cc/g	0.4858 cc/g

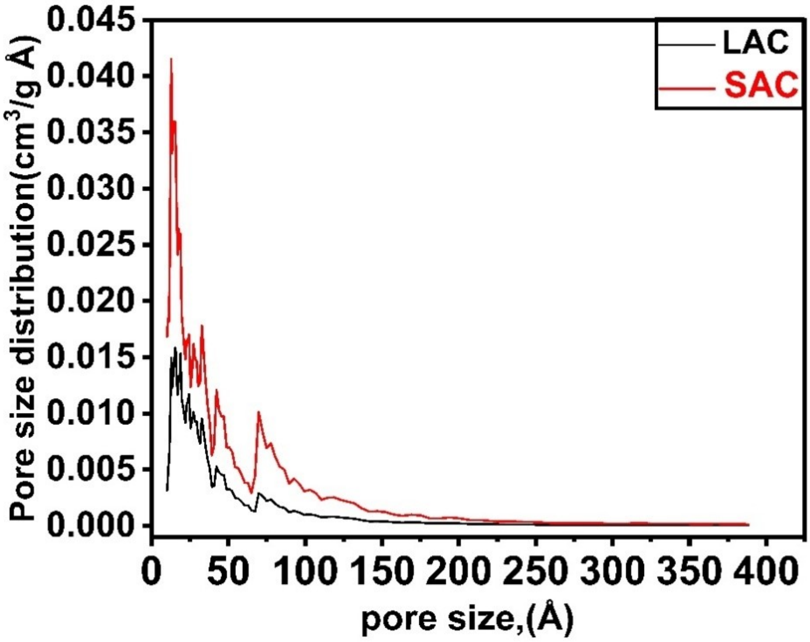

Figure S1. Pore size distribution of SAC and LAC

Results

			Mean (mV)	Area (%)	St Dev (mV)
Zeta Potential (mV):	-10.4	Peak 1:	-10.4	100.0	5.72
Zeta Deviation (mV):	5.72	Peak 2:	0.00	0.0	0.00
Conductivity (mS/cm):	0.110	Peak 3:	0.00	0.0	0.00
Result quality :	Good				

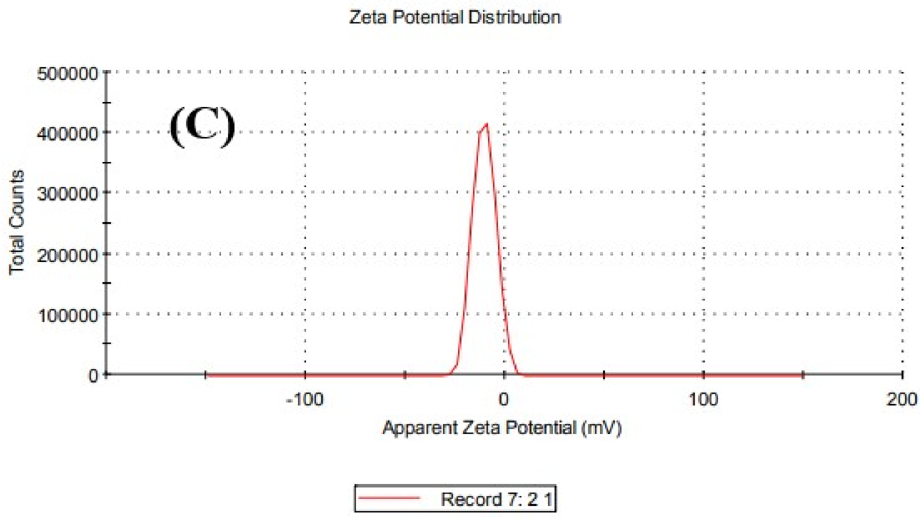

Figure S2. Zeta potential of SAC.

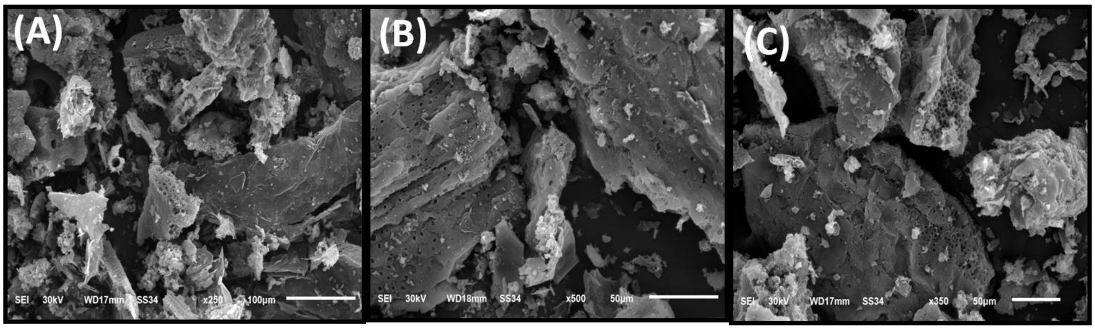

Figure S3: SEM images of SAC (A-C).

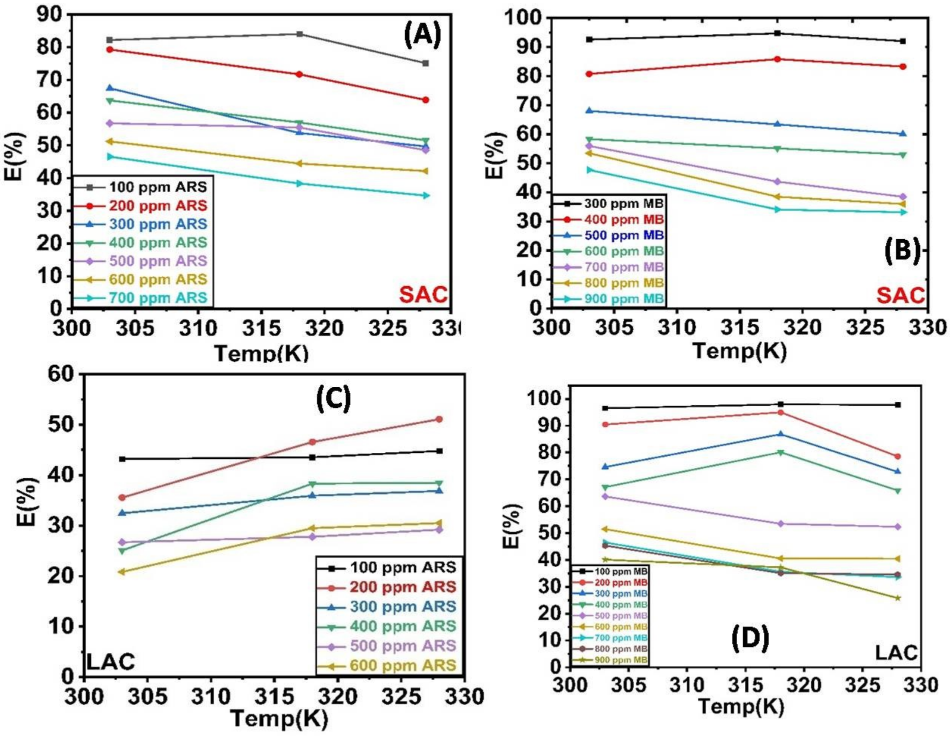

Figure S4: Effect of temperature on the removal of MB and ARS dyes using LAC and SAC.

S1:

The PFO model usually predicts the behavior at the initial stage of the adsorption process, while PSO model predicts the behavior at all stages of the adsorption process[1].

Pseudo-first-order kinetic model:

$$\log\left(q_e - q_t\right) = \log q_e - \frac{K_1\, t}{2.303} \qquad (1)$$

Pseudo-second-order kinetic model:

$$\frac{t}{q_t} = \frac{1}{K_2 {q_e}^2} + \frac{t}{q_e} \qquad (2)$$

Where k_1 (min^{-1}) and k_2 (g mol^{-1} min^{-1}) are the rate constants. q_t and q_e are the adsorption uptake of heavy metal at time t (min) and at equilibrium. Where k_1 (min^{-1}) and k_2 (g mol^{-1} min^{-1}) are the rate constants. q_t and q_e are the adsorption uptake of heavy metal at time t (min) and at equilibrium.

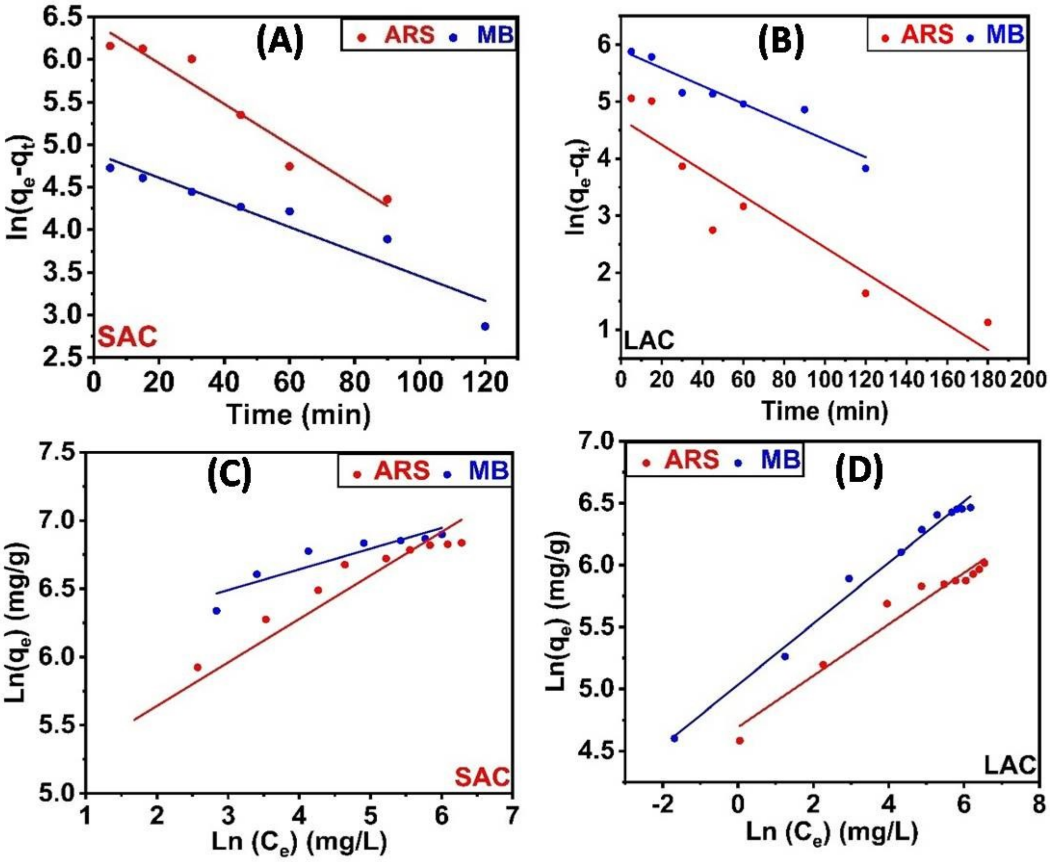

Figure S5: PFO kinetic models for the adsorption of MB and ARS onto SAC (A) and LAC (B); Freundlich isotherm model for the adsorption of MB and ARS onto SAC (C) and LAC (D).

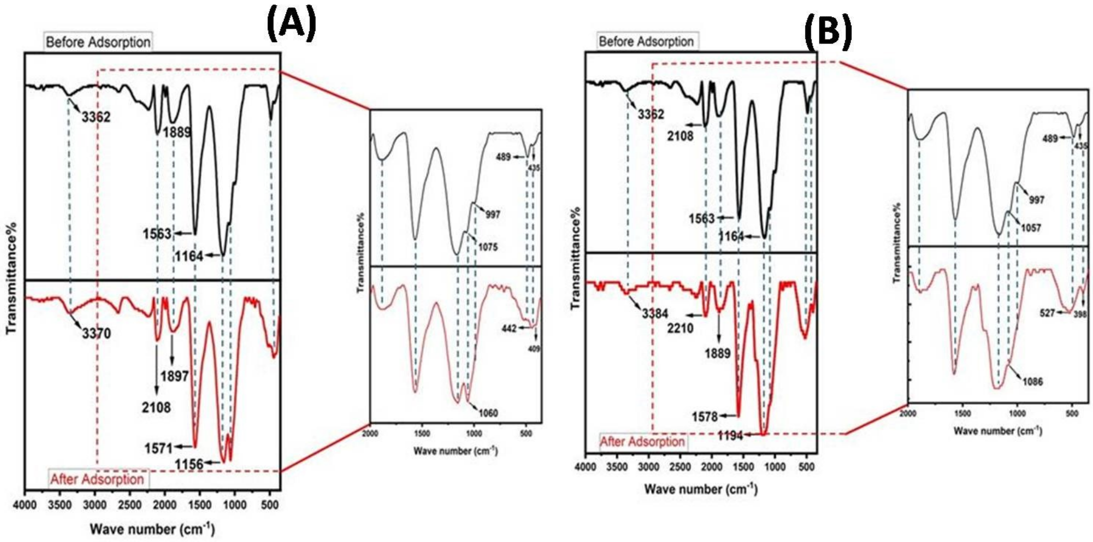

Figure S6: FTIR spectra of SAC Before and after MB adsorption (A) and ARS adsorption.

References

[1] A.M. El-Wakil, S.M. Waly, W.M. Abou El-Maaty, M.M. Waly, M. Yılmaz, F.S. Awad, Triazine-Based Functionalized Activated Carbon Prepared from Water Hyacinth for the Removal of Hg2+, Pb2+, and Cd2+ Ions from Water, ACS omega 7(7) (2022) 6058-6069.